



HAL
open science

A tailored approach to optimize the barrier properties of Poly(lactic acid) nanocomposites for food contact purposes

Xiaoyi Fang, Olivier Vitrac, Sandra Domenek, Violette Ducruet

► To cite this version:

Xiaoyi Fang, Olivier Vitrac, Sandra Domenek, Violette Ducruet. A tailored approach to optimize the barrier properties of Poly(lactic acid) nanocomposites for food contact purposes. *Matériaux 2010*, Fédération Française des Matériaux (FFM), Oct 2010, Nantes, France. pp.10. hal-01173790

HAL Id: hal-01173790

<https://hal.science/hal-01173790>

Submitted on 4 Jun 2020

HAL is a multi-disciplinary open access archive for the deposit and dissemination of scientific research documents, whether they are published or not. The documents may come from teaching and research institutions in France or abroad, or from public or private research centers.

L'archive ouverte pluridisciplinaire **HAL**, est destinée au dépôt et à la diffusion de documents scientifiques de niveau recherche, publiés ou non, émanant des établissements d'enseignement et de recherche français ou étrangers, des laboratoires publics ou privés.

A tailored approach to optimize the barrier properties of Poly(lactic acid) nanocomposites for food contact purposes

Xiaoyi Fang, Olivier Vitrac*, Sandra Domenek, Violette Ducret

Joint Research Unit 1145 Food Process Engineering between Agroparistech and INRA
1, avenue des Olympiades, 91300 Massy, France.

ABSTRACT:

A new kind of barrier materials, so called “chaotic” materials and involving interactions with nano-charges, is presented. By contrast with conventional use of nano-clays, the sought effect consists not in increasing the tortuosity to penetrants but in increasing the dwelling times of solutes around accessible clays designed on purpose. The paper reviews several theoretical models that explain why effective diffusion coefficients (D) decay due to entropic trapping. The physical concepts are applied to a simple material made of a deactivated glass column filled with montmorillonites and exposed to several gas phases enriched in organic solutes. In this simple physical model, a carrier gas replaces the polymer so that molecular effects can be visualized and analyzed almost in real time with a simple flame-ionization detector. The future directions to combine a bio-sourced material (PLA) and montmorillonites are outlined.

KEYWORDS: *diffusion, nano-material, thermodynamics, inverse gas chromatography*

1 INTRODUCTION

Barrier polymer materials is of high importance in many areas including modified atmosphere packaging[1], materials with low leaching and therefore low food safety issues[2], polymer ageing[3], membrane separation[4]. Usually, good barrier polymer materials combine high cohesive energy density (e.g. glassy in conditions of use) and/or possibly an oriented crystalline fraction. [5-8] When intrinsic properties do not match expectation, a combination of materials (composite materials) must be used. Such strategies usually do match however current requirements for environment-friendly materials that do not use non-renewable carbon sources, and/or that are recyclable for the same purpose (e.g. food contact) or biodegradable. Due to their high sensitivity of water and other food constituents, current bio-sourced materials fails to provide good alternative to synthetic food contact materials when good barrier properties are desirable. [9-11] In this perspective, we argue that the paradigm of materials opposing low diffusivity to penetrants need to be revised, while integrating last comprehension of molecular transport in polymers for gas, volatile and non-volatile penetrants. Two concepts are particularly appealing: materials with reactive barriers and “chaotic” materials. The first kind of materials has been initially developed in the 1970s for groundwater and soils remediation (i.e. reduction of chlorinated contaminants, reductive precipitation and immobilization of uranium, chromium, and arsenic) [12]. It has been extended independently to chemical reactive packaging materials that incorporates a layer capable of removing (scavenging) a permeating species. [13] As existing scavengers are mainly focused on oxygen and water, their application to broad range of penetrants in particular organic substances is still speculative. “Chaotic materials” follow a different route and rely on a molecular description of penetrant random walks. By controlling the fractal trajectory of penetrants, the conventional white-noise Brownian motion of penetrants on short time scales can be replaced by color-chaos noise that incorporates some correlated motions. [14] The relationship between the spread of polymer-penetrant-free energies at molecular scale, correlations in penetrant displacements and finally decrease in diffusion coefficients, D, has been investigated by one of us[15]. It has been demonstrated theoretically that D values might be decreases by several decades by increasing locally the chemical affinity for some accessible regions in the polymer regardless their topological organization. Combined with molecular modeling of excess chemical potentials[16-18], such findings could be used to design novel materials that are barrier to specific organic penetrants. We are

* Corresponding author

currently developing a prototype of such “chaotic” materials barrier to lipophilic food constituents (fat-contents, aroma...) based on a polylactic acid (PLA), a biodegradable polymer[9], and specifically-modified montmorillonites, used a local chemical potential modifier. Both polymer and charge types were selected because an important literature has been generated on methodologies to process such materials, see in particular the reviews in references[19-27].

The goal of this communication is to present the principles of such materials from both theoretical considerations and simple macroscopic experiments that reproduce expected effects. The paper is organized as follows. Section two reviews existing and novel theories of diffusion involving entropic trapping. Section three presents simple experimental results based on inverse gas chromatography (IGC), which simulates “chaotic” materials while preserving some main ingredients: molecular interactions at the surface of mineral clays. In particular, it is shown that replacing partly diffusion by convection within a dense porous media make it possible to reproduce experimentally phenomena that would require weeks or months in PLA at room temperature. Future extensions and validations are finally discussed in the last section.

2 THEORY OF PASSIVE BARRIER MATERIALS

This section reviews existing thermodynamical concepts and strategies to tune transport properties of polymer materials regardless their initial physico-chemical properties. A complementary full mechanistic point of view of trace diffusion in an amorphous polymer based on long-term molecular dynamics simulations can be found in[28].

2.1 EXISTING BARRIER MATERIALS

When intrinsic properties do not match expectation, a combination of materials must be considered such as multilayers (composite materials) or nanoclays materials (nano-composite).

2.1.1 Multilayer materials

In multilayer materials, mass transport resistances are additive with each uniform layer j opposing to penetrants a resistance $\mathfrak{R}_j = \frac{l_j k_j}{D_j}$, where l_j , k_j and D_j are respectively the thickness, the Henry coefficient

(reciprocal solubility) and diffusion coefficient respectively. In presence of microscopic gradient of properties, a more general formalism derived either from irreversible thermodynamics or from Stefan-Maxwell approach[29]. The driving force of mass transfer is a chemical potential gradient instead of a concentration gradient, both are related from the Gibbs relationship and the sorption isotherm. Along dimension x , one gets:

$$\frac{\partial \mu}{\partial x} = \frac{\partial \mu}{\partial X} \frac{\partial X}{\partial x} = RT \frac{\partial \ln(\gamma X)}{\partial X} \frac{\partial X}{\partial x} = \frac{RT}{C} \left[\frac{\partial \ln(\gamma)}{\partial \ln(X)} + 1 \right] \frac{\partial C}{\partial x} \quad (1)$$

with γ , X , C being the activity coefficient, the molar fraction and the volume concentration in penetrants. R is the ideal gas constant and T is absolute temperature.

By replacing in the first Fick's equation the concentration gradient by the generalized driving force defined in Eq. (1), the diffusive flux of penetrants j may be thought as resulting from a force balance between driving forces (due to thermal agitation or macroscopic gradients) and viscous frictions with the surrounding medium:

$$-\frac{\partial \mu}{\partial x} = \frac{RT}{D} \underbrace{\left(\frac{d \ln \gamma}{d \ln X} + 1 \right)}_{\Gamma} \frac{j}{C} = \frac{RT}{D} \Gamma (v - v^{\text{bulk}}) = \xi (v - v^{\text{bulk}}) \quad (2)$$

where $v - v^{\text{bulk}}$ is the penetrant net velocity relative to the bulk phase, Γ is a thermodynamic correction factor (to account for non idealities). ξ is a friction coefficient that generalizes the Einstein relation used in kinetic theory as $D = \Gamma \frac{RT}{\xi}$. Molar coatings, plasma-surface treatments and other layered nanoarchitecture methods provide opportunities for creative design and application of new barrier materials [30,31].

2.1.2 Nano-clay materials: simple “chaotic” materials

The lengthening of diffusion path by adding obstacles is known to decrease the diffusion coefficient. By noting the tortuosity factor ζ (i.e. factor of increase of diffusion path), lumped diffusion coefficient D_e becomes by analogy with porous media [32]:

$$D_e = \frac{D}{\zeta} \epsilon \quad (3)$$

with ϵ is the relative open cross-sectional area open to diffusion and D being the diffusion coefficient in the homogeneous material. Reduction of D is maximized when obstacles present large sections oriented perpendicular to the direction of transfer. Elastomeric-clay nanocomposites have been reviewed in [33]. Additional effects could be gained by introducing a fractal description diffusion coefficient [**Error! Bookmark not defined.**]. Indeed, the effect of additional zigzags in the random walk of diffusants must be envisioned as negative correlations impeding the mean square displacements, $\left\langle \mathbf{r}(t, 2^k \tau) \cdot \mathbf{r}(t, 2^k \tau) \right\rangle_{\text{all } t}$, visited by the penetrant on different time scales $2^k \tau$:

$$\begin{aligned} \left\langle \mathbf{r}(t, 2^k \tau) \cdot \mathbf{r}(t, 2^k \tau) \right\rangle_{\text{all } t} &= 2 \left\langle \mathbf{r}(t, 2^{k-1} \tau) \cdot \mathbf{r}(t, 2^{k-1} \tau) \right\rangle_{\text{all } t} (1 + \cos \theta_{k-1}) \\ &= 2^k \left\langle \mathbf{r}(t, \tau) \cdot \mathbf{r}(t, \tau) \right\rangle_{\text{all } t} \prod_{i=0}^{k-1} (1 + \cos \theta_i) \end{aligned} \quad (4)$$

where $\mathbf{r}(t, \tau)$ is the displacement vector between t and $t+\tau$, $\cos \theta_i$ is the averaged angle between displacements observed at time scale $2^i \tau$. Operators $\left\langle \right\rangle_{\text{all } t}$ and \cdot denote ensemble average over all possible starting times and scalar product. By noticing that $D(2^i \tau) \simeq \frac{1}{6} \left\langle \mathbf{r}(t, 2^i \tau) \cdot \mathbf{r}(t, 2^i \tau) \right\rangle / 2^i \tau$, one gets:

$$\frac{1}{k \ln 2} \sum_{i=0}^{k-1} \ln(1 + \cos \theta_i) = \int_{\tau}^{2^k \tau} \left(\frac{d \ln \left\langle \mathbf{r}(t, \tau) \cdot \mathbf{r}(t, \tau) \right\rangle_{\text{all } t}}{d \ln \tau} - 1 \right) d\tau \simeq \ln \frac{D(2^k \tau)}{D(\tau)} \quad (5)$$

Eq. (5) demonstrates that within a “chaotic” material, effects on tortuosity could be combined on several time scales by accumulating correlations on a log-time scale (conditions of pink noise).

2.2 GENERALIZED “CHAOTIC” MATERIALS INVOLVING ENTROPIC TRAPPING

Entropic trapping emerges spontaneously as soon as molecular translation occurs on a rough potential energy surface. The most visible consequence is that diffusant spends most of its time near the minima and occasionally jumps over the potential maxima. The resulting heterogeneous Poissonian dynamics has been evidenced both on molecular dynamics simulations in polymers[34,28] and on particle transport on disordered lattices[35,36,15].

2.2.1 Trapping subjected to a single well

Effects of correlated displacements, or equivalently between velocities $v(t)$, are appraised via the Green-Kubo relation:

$$\frac{d}{d\tau} \langle \mathbf{r}(t, \tau) \cdot \mathbf{r}(t, \tau) \rangle_{\text{all } t} = 2 \int_0^\tau \left\langle \frac{d\mathbf{r}}{d\tau}(t + \kappa) \cdot \frac{d\mathbf{r}}{d\tau}(t) \right\rangle_{\text{all } t} d\kappa = 2 \int_0^\tau \langle \mathbf{v}(t + \kappa) \cdot \mathbf{v}(t) \rangle_{\text{all } t} d\kappa = 6D(\tau) \quad (6)$$

When diffusant velocity correlation obeys to a linear damping law with a time constant τ_0 , $D(\tau)$ increases as $D(0)(1 - \exp(-\tau/\tau_0))$. In presence of trapping, the variation is opposite and D is found decreasing. As suggested in [37], one convenient picture is to think about a punctual particle undergoing a true random walk (non-correlated motions) within an empty sphere (geometrical constraints). The particle is expected to collide periodically with the wall so that velocity will appear opposite as depicted in Fig. 1b. In practice no starting time needs to be privileged (stationary condition) and the time interval between two collisions is consequently given by the ratio between the sphere diameter and the particle velocity. For a true random walk, impinging times obeys to the reciprocal Maxwell-Boltzmann distribution depicted in Fig. 1a. The corresponding velocity correlation functions and D variations are plotted in Fig. 1c and 1d respectively. It is worth to notice that the limit D value goes down to zero for a perfectly trapped molecule. As molecules are non-permanently trapped in IGC, the effect of dragging (as performed in IGC) is also represented by introducing an asymmetric trapping (periods with positive correlations are 5% longer than with negative correlations). In the latter case, the variation of D is non monotonous and dragging dominates long-term transport.

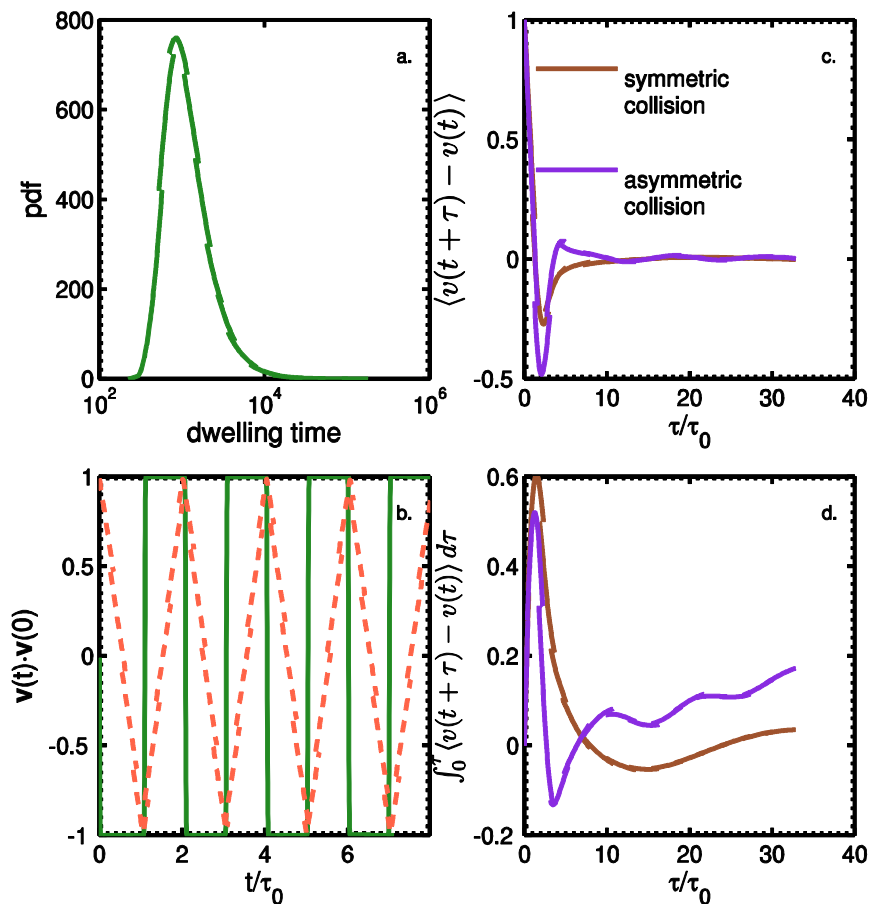


Figure 1. Dynamics of a particle moving randomly within a sphere. (a) Distribution of collision times (reciprocal of a Maxwell-Boltzmann distribution). (b) Velocity correlations for a particular starting position (continuous line) and averaged over all possible starting times (dashed line). (c) Velocity correlations averaged all collision intervals. (d) Corresponding 3D(τ) values.

The friction coefficient defined in Eq. (2) accepts a microscopic interpretation as a memory function in Langevin equation:

$$\frac{d}{d\tau} \left\langle \mathbf{v}(t + \kappa) \cdot \mathbf{v}(t) \right\rangle_{\text{all } t} = - \int_0^{\tau} \xi(\tau - \kappa) \left\langle \mathbf{v}(t + \kappa) \cdot \mathbf{v}(t) \right\rangle_{\text{all } t} d\kappa \quad (7)$$

2.2.2 Trapping subjected to multiple wells

In the limit of intermediate to strong friction (the time spend to escape the well is much longer than the time to move from one well to the next one), the corresponding kinetic obeys to transition state theory. This sub-section introduced a simplified version of multiple transitions studied by us[15]. By assuming that molecular transport occurs between two types of adjacent wells as depicted in Fig. 2, the relationship between probabilities of occupancy, $p_{eq}^{c \text{ or } d}$, and frequencies of hopping, $k_{c \rightarrow d}$ or $k_{d \rightarrow c}$, are given at thermodynamical equilibrium by the detailed mass balance:

$$p_{eq}^c k_{c \rightarrow d} = p_{eq}^d k_{d \rightarrow c} \quad (8)$$

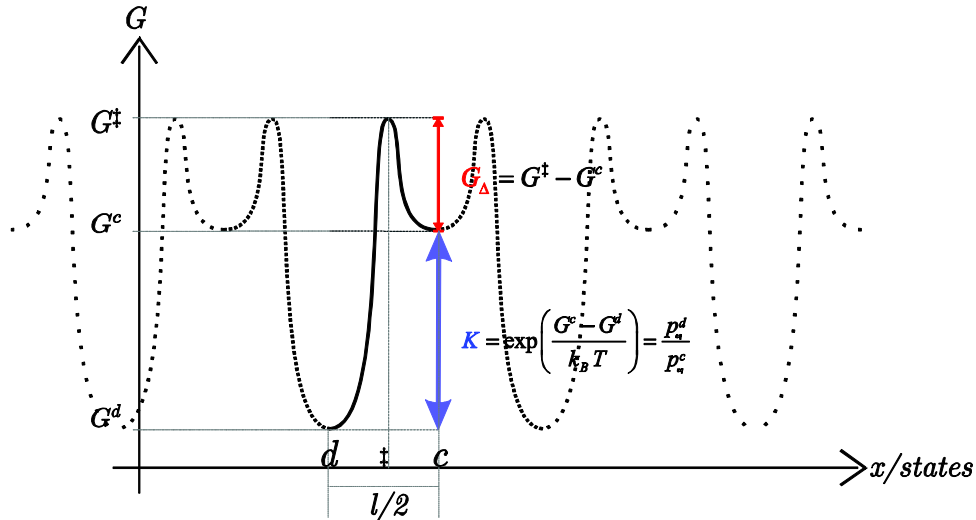


Figure 2. Mass transport along a periodic free-energy 1D profile, where typical sites c and d are separated by a distance $l/2$. \ddagger represents the transition state to cross from one site to next one.

By writing transition frequency as $k_{A \rightarrow B} = k_0 \exp\left(\frac{G^A - G^\ddagger}{RT}\right)$, the corresponding diffusion coefficient is shown to decrease with the ratio of probability $K = p_{eq}^c / p_{eq}^d$:

$$2D = l^2 k_{d \rightarrow s \rightarrow d} = \frac{l^2}{(k_{d \rightarrow c})^{-1} + (k_{c \rightarrow d})^{-1}} = \frac{k_0 l^2}{\frac{K}{\exp\left(-\frac{G_\Delta}{RT}\right)} + \frac{1}{\exp\left(-\frac{G_\Delta}{RT}\right)}} = \frac{k_0 l^2}{1 + K} \exp\left(-\frac{G_\Delta}{RT}\right) \quad (9)$$

3 IGC AS A SIMPLE EXAMPLE OF CHAOTIC MATERIALS

3.1 STEADY-STATE TRANSPORT AT THE SCALE OF SINGLE SORPTION SITE

The steady transport of a population of penetrants at the scale of one single sorption site along the column is idealized in Figure 3. The longitudinal direction represents a macroscopic transport along the column with nitrogen as carrier gas, while the transverse direction details the mass balance at molecular scale. The residence time of each penetrant at the site position depends strongly whether it will interact or not with the surface. The whole process is described as a jumping process with frequencies k_g , k_a and k_d . Corresponding mass fluxes, f_g , f_a and f_d , are defined as the product of the upstream concentration with frequency. The microreversibility at the scale of the sorption site (condition of local thermodynamical equilibrium) enforces $f_s=f_g$. At any time, the molar fraction in gas and solid phases, denoted $m_g\%$ and $m_s\%$ respectively, are:

$$m_g\% = \frac{c_g k_g}{c_g (k_g + k_a)}; m_s\% = \frac{c_s k_d}{c_g (k_g + k_a)} = \frac{c_s k_a}{c_g (k_g + k_a)} \quad (10)$$

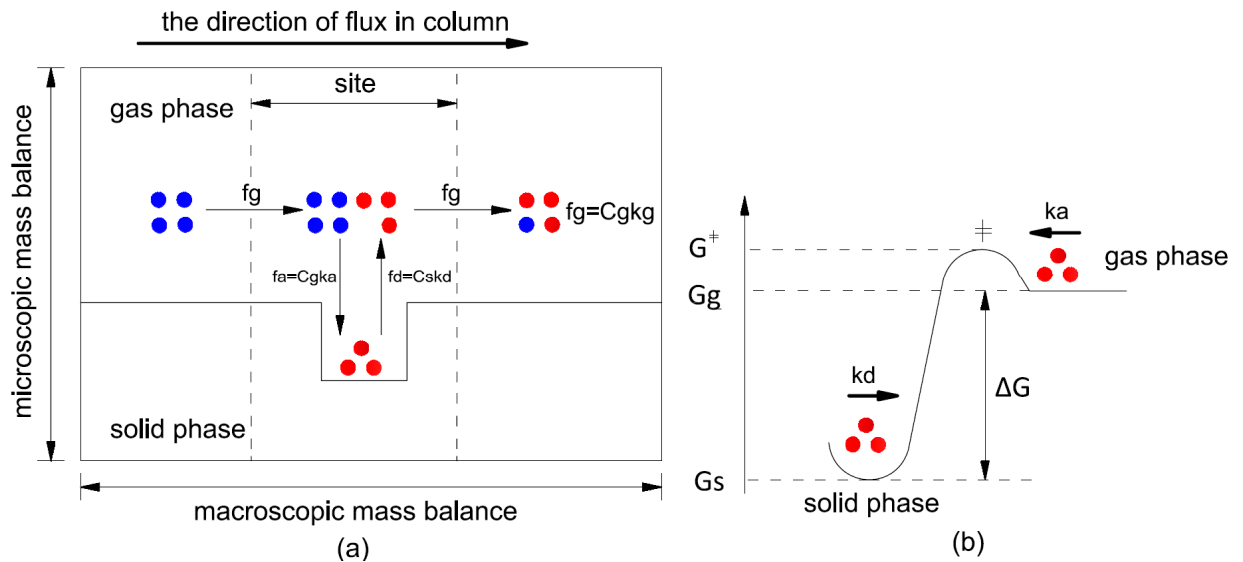


Figure 3. (a) The mass transfer description at one site in the column of IGC. (b) The free energy distribution in the process of desorption.

The residence time is finally averaged between the residence times of adsorbed and non-adsorbed populations as:

$$t_R^{site} = \frac{1}{k_g} \frac{c_g k_g}{c_g (k_g + k_a)} + \left(\frac{1}{k_d} + \frac{1}{k_g} \right) \frac{c_s k_a}{c_g (k_g + k_a)} = \frac{1}{k_g + k_a} \left(1 + \frac{k_a}{k_d} + \frac{k_a}{k_g} \right) \quad (11)$$

3.2 THERMODYNAMICAL INTERPRETATION

It is emphasized that Eq. (11) is valid either when the continuous phase is a gas or a polymer. In presence of a gas phase, additional simplifications can be obtained by noting that $k_g \gg k_a$ and $k_g \gg k_d$ and one gets for a column including N sites:

$$t_R = \sum_{i=1}^N t_R^{site} = \frac{N}{k_g} \left(1 + \frac{k_a}{k_d} \right) = t_R^{ref} \left(1 + \frac{k_a}{k_d} \right) \quad (12)$$

with t_R^{ref} being the residence time for a substance non-interacting with the surface but possibly subjected to tortuosity effects in the column. In our experiments, we used methane to determine this reference time. The specific dwelling time due to specific interaction with the surface was expressed in the framework of the transition state theory (see section 2.2.2 and Figure 3b):

$$\frac{t_R - t_R^{ref}}{t_R^{ref}} = \frac{k_a}{k_d} = \frac{k_o \exp\left(-\frac{G^\ddagger - G_g}{RT}\right)}{k_o \exp\left(-\frac{G^\ddagger - G_s}{RT}\right)} = \exp\left(\frac{G_g - G_s}{RT}\right) = \exp\left(\frac{\Delta G}{RT}\right) = \exp\left(\frac{\Delta H}{RT} - \frac{\Delta S}{R}\right) \geq 1 \quad (13)$$

A direct measurement of free energies due to adsorption is not possible but from the dependence of $\ln\left(t_R/t_R^{ref} - 1\right)$ with $1/T$, both enthalpic and entropic contributions can be derived.

3.3 EXPERIMENTAL EVIDENCES FOR N-ALKANES

Retention times for a homologous series of n-alkanes ranging from pentane (C5) to nonane (C9) were measured to validate the principles of “chaotic” materials in various experimental conditions. The proposed “chaotic” material consisted in 117 mm long deactivated glass column (inner diameter 8 mm) filled with dried Na⁺-montmorillonite (reference cloisite Na⁺, South Clay Products, USA). Concentrations were measured at the outlet of the column using a flame-ionization detector. Methane (C1) was used as reference to assess the non-thermodynamically controlled retention time. Results are summarized in Figure 4. Distributions of retention times were highly asymmetric and match accordingly the reciprocal Maxwell-Boltzmann distribution (compare Figures 1a and 4a). Although a carrier gas was used, it evidenced that random walk through the porous structure controlled the spread of retention times regardless the applied carrier gas flow rate. The practical consequence is that two typical retention times could be calculated: the most probable retention time (distribution mode) and the averaged retention time. Both quantities were partly linearly correlated but the later tented to give larger values (Figure 4b). Specific tests with variable flow rates demonstrated that both $t_R/t_R^{ref} - 1$ was unaffected by the macroscopic mass transport in the gas phase and that the considered adsorption isotherm was linear with the concentration in the gas phase (Figure 4c). In addition, it was confirmed that $t_R/t_R^{ref} - 1$ followed an Arrhenian behavior with a slope (ΔH) increasing slightly with the number of carbons, as expected from pure van-der-Walls interactions (Fig. 4d). It is however highlighted that the values of enthalpies depended on the considered value of retention times. Retention times at maxima of probability led to more accurate Van-Hoff plots but ensemble-averages must be preferred for a consistent thermodynamical interpretation.

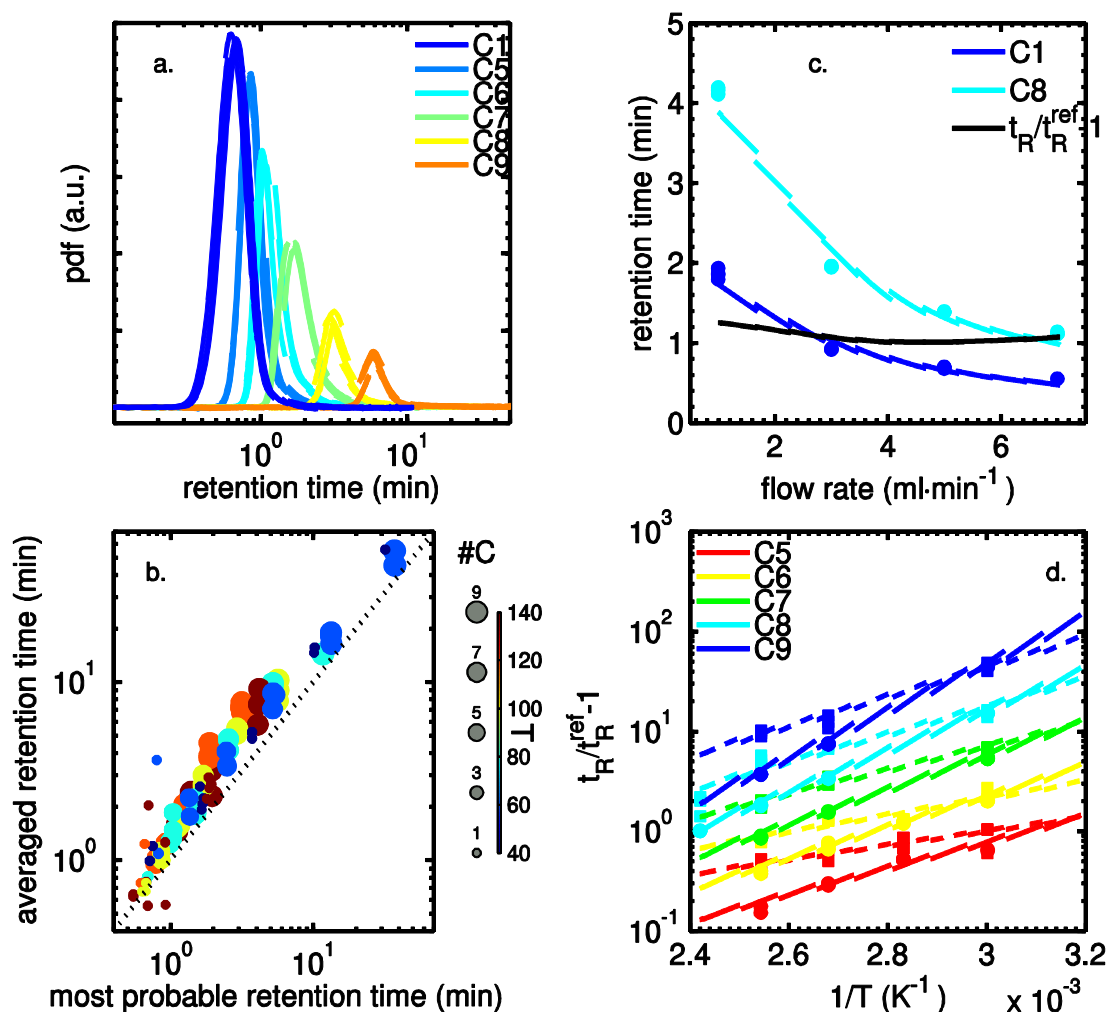


Figure 4. Experimental results obtained in inverse gas chromatography (injection volume ca. $0.02 \mu\text{l}$). (a) retention times at 100°C . (b) Crude comparisons with 134 experimental conditions. (c) Nitrogen flow rate effect at 140°C . (d) Van-Hoff plots of $t_R/t_R^{\text{ref}} - 1$.

4 CONCLUSIONS

The principles of “chaotic” materials has been presented and illustrated on a porous material packed into a chromatographic column. By replacing the polymer continuous phase by a carrier gas, the analogous system made it possible to assess efficiently the effects of molecular interactions on effective transport properties for organic solutes. Such effects will be used in a next step to design PLA-based materials that are specifically barriers to similar organic substances. The most promising direction consists in modifying the surface of studied montmorillonite clays to optimize the difference in excess chemical potentials between PLA and platelet surfaces. It is worth to notice that described barrier effects are cumulative to already described technological effects aiming at increasing the tortuosity in polymer based nano-materials. In this work, resistance to diffusion controlled by both tortuosity and dead-end effects appears as significantly asymmetric retention time distributions that can be fit with conventional Maxwell-Boltzmann distribution. Similar results were obtained by modeling the mass transport within the column as a result of both convection and diffusion (see [38] for more details):

$$\delta \frac{\partial c}{\partial t} + \nabla \cdot (-D \nabla c + c \mathbf{u}) = 0 \quad (14)$$

where c is concentration and \mathbf{u} is carrier gas velocity vector. Capacitance parameter δ scales the retention time distribution, it is equal to 1 in absence of interactions with the material in the column and higher than 1 otherwise. It is thus shown that diffusion in the bulk (controlled by D) and molecular interactions at the surface of clays (controlled by δ) describe distinct effects. In absence of convection ($\mathbf{u} = \mathbf{0}$), effective transport equation becomes equivalent to a second Fick's equation (or Fokker-Planck equation) with an effective diffusion coefficient, D_{eff} , combining both D and δ :

$$\frac{\partial c}{\partial t} = \nabla \cdot \left(\frac{D}{\delta} \nabla c \right) = \nabla \cdot (D_{eff} \nabla c) \quad (15)$$

Equation (15) could define is a "chaotic" material is within the continuous mechanics framework. It is worth to notice that D_{eff} should not be confused with a permeability as driving forces in diffusive flux are expressed as concentration gradients and not as pressure gradients.

5 REFERENCES

1. J. D. Floros and K. I. Mastos. Introduction to modified atmosphere packaging. In "Innovations in Food Packaging". Academic Press, 2005. 159-172.
2. O. Vitrac and M. Hayert. Risk assessment of migration from packaging materials into foodstuffs. *AIChE J.*, 51:1080–1095, 2005.
3. K. Pielichowski and J. Njuguna. Thermal Degradation of Polymeric Materials. Rapra Technology Ltd, 2005. 306p.
4. S. Pereira Nunes and K.-V. Peinemann. Membrane technology in the chemical industry, 2nd Edition. Wiley-VCH, 2006. 354p.
5. A. Alentiev and Y. Yampolskii. Prediction of gas permeation parameters of polymers. In "Materials Science of Membranes for Gas and Vapor Separation". Ed. Y. Yampolskii, I. Pinnau and B. D. Freeman. John Wiley & Sons, 2006, 211-229.
6. L. H. Sperling. Chapter 4 : concentrated solutions, phase separation behavior and diffusion. In "Introduction to Physical Polymer Science". John Willey & Sons, 2006, 146-195.
7. J. Bicerano. Transport of small penetrant molecules. In "Prediction of Polymer Properties. 3rd Ed.". Marcel Dekker Inc., 2002, Chapter 15.
8. S. A. Ster, and J. R. Fried. Permeability of polymers to gases and vapors. In "Physical properties of polymers handbook. 2nd Edition". Springer Science, 2007, 1033-1047.
9. Handbook of biodegradable polymers. Ed. A. J. Domb, J. Kost and D. M. Wiseman. Overseas Publishers Association, Amsterdam, 1997. 510p
10. R.M. Johnson, L.Y. Mwaikambo and N. Tucker. Biopolymers. Rapra review report 2003, 14(3), Report 159. 147p
11. R. A. Auras. Chapter 19 : solubility of gases and vapors in polylactide polymers. In "Thermodynamics, Solubility and Environmental Issues". Ed. T.M. Letcher, Elsevier B.V., 2007, 343-368.
12. M. C. Lo and K. C. K. Lai. Chemical Reactive barriers. In "Remediation Technologies for Soils and Groundwater". Ed. American Society of Civil Engineers, 2007. 177-198.
13. S. Solovyov and A. Goldman, Mass transport and reactive barriers in packaging. Destech Publications. 2008. 541p.
14. R. Klages. Microscopic chaos, fractals and transport in nonequilibrium statistical mechanics. World Scientific. 2007. 441p.
15. O. Vitrac and M. Hayert. Effect of the distribution of sorption sites on transport diffusivities: A contribution to the transport of medium-weight-molecules in polymeric materials. *Chemical Engineering Science* 2007, 62(9), 2503–2521.
16. G. Gillet, O. Vitrac and S. Desobry. Prediction of Solute Partition Coefficients between Polyolefins and Alcohols Using a Generalized Flory–Huggins Approach. *Industrial Engineering Chemistry Research* 2009, 48(11), 5285–530.

17. G. Gillet, O. Vitrac and S. Desobry. Prediction of Partition Coefficients of Plastic Additives between Packaging Materials and Food Simulants. *Industrial Engineering Chemistry Research* 2010, 10.1021/ie9010595
18. O. Vitrac and G. Gillet. An Off-Lattice Flory-Huggins Approach of the Partitioning of Bulky Solutes between Polymers and Interacting Liquids. *International Journal of Chemical Reactor Engineering* 2010, 8, A6.
19. Perrine Bordes, Eric Pollet and Luc Avérous. Nano-biocomposites: Biodegradable polyester/nanoclay systems. *Progress in Polymer Science*. 2009, 34, 125-155.
20. Suprakas Sinha Ray and Mosto Bousmina. Biodegradable polymers and their layered silicate nanocomposites: In greening the 21st century materials world. *Progress in Materials Science*. 2005,50,962-1079.
21. M. Pluta, A. Galeski, M. Alexandre, M.-A. Paul, P. Dubois. Poly(lactide)/montmorillonite nanocomposites and microcomposites prepared by melt blending: Structure and some physical properties. *Journal of Applied Polymer Science*. 2002,86,1497-1506.
22. Jin-Hae Chang, Yeong Uk An, Gil Soo Sur. Poly(lactic acid) nanocomposites with various organoclays. I. Thermomechanical properties, morphology, and gas permeability. *Journal of Polymer Science Part A: Polymer Chemistry*. 2002, 41, 94-103.
23. Henriette M.C. de Azeredo. Nanocomposites for food packaging applications. *Food Research International*. 2009, 42, 1240-1253.
24. Marie-Amélie Paul, Michaël Alexandre, Philippe Degée, Cédric Calberg, Robert Jérôme, Philippe Dubois. Exfoliated Poly(lactide)/Clay Nanocomposites by In-Situ Coordination-Insertion Polymerization. *Macromolecular Rapid Communications*. 2003, 24, 561-566.
25. Marie-Amélie Paul, Cécile Delcourt, Michaël Alexandre, Philippe Degée, Fabien Monteverde, André Rulmont, Philippe Dubois. (Plasticized) Poly(lactide)/(Organo-)Clay Nanocomposites by in situ Intercalative Polymerization. *Macromolecular Chemistry and Physics*. 2005, 206, 484-498.
26. Vahik Krikorian and Darrin J. Pochan. Poly (l-Lactic Acid)/Layered Silicate Nanocomposite: Fabrication, Characterization, and Properties. *Chem. Mater.*, 2003, 15, 4317-4324.
27. Tzong-Ming Wu and Cheng-Yang Wu. Biodegradable poly(lactic acid)/chitosan-modified montmorillonite nanocomposites: Preparation and characterization. *Polymer Degradation and Stability*. 2006, 91, 2198-2204.
28. M. Durand, H. Meyer, O. Benzerara, J. Baschnagel, and O. Vitrac. Molecular dynamics simulations of the chain dynamics in monodisperse oligomer melts and of the oligomer tracer diffusion in an entangled polymer matrix. *Journal of Chemical Physics* 2010, 132:194902.
29. R. Krishna and J. A. Wesselingh, The Maxwell-Stefan approach to mass transfer. *Chemical Engineering Science* 1997, 52(66), 861-911.
30. J. B. Schlenoff. Charge Balance and Transport in Polyelectrolyte Multilayers. In "Multilayer Thin Films Sequential Assembly of Nanocomposite Materials", Ed. G. Decher, J. B. Schlenoff. Wiley-VCH Verlag, 2002, 99-132.
31. D. Nicholson and N. Quirke. Adsorption and transport at nanoscale. In "Adsorption and Transport at the Nanoscale", Ed. N. Quirke, CRC Press, 2006, 1-14.
32. D. Basmadjian. Mass transfer : principles and applications. CRC Press, 2005. p 110
33. S. D. Sadhu, M. Maiti and A. K. Bhowmick. Elastomer-clay nanocomposites. In "Current Topic in Elastomers reserach". Ed. A. K. Bhowmick, CRC Press , 2008, 23-56.
34. A.Gusev and U. W. Suter. Dynamics of small molecules in dense polymers subject to thermal motion. *Journal of Chemical Physics* 1993, 99:2228-2234.
35. K. Kundu and P. Phillips. Hopping transport on site-disordered d-dimensionallattices. *Physical Review A* 1987, 35, 857-865; J. W. Haus and K. W. Kehr. Particle transport on d-dimensional disordered lattices. *ibid.* 1988, 37, 4522-4523; K. Kundu and P. Phillips. Reply to Particle transport on d-dimensional disorderly lattices. *ibid.* 37 1988, 4524-4525.
36. N. C. Karayiannis, V.G. Mavrantzas, and D. N Theodorou. Diffusion of small molecules in disordered media: study of the effect of kinetic and spatial heterogeneities. *Chemical Engineering Science* 2001, 56:2789-2801.
37. D. R. Rottach, P. A. Tillman, J. D. McCoy, S. J. Plimpton and J. G. Curro. The diffusion of simple penetrants in tangent site polymer melts. *Journal of Chemical Physics* 1999, 111, 9822-9831.
38. A. Cavazzini, F. Dondi, A. Jaulmes, C. Vidal-Madjar and A. Felinger. Monte Carlo model of nonlinear chromatography: correspondence between the microscopic stochastic model and the macroscopic Thomas kinetic model. *Analytical Chemistry* 2002, 75, 6269-6278.